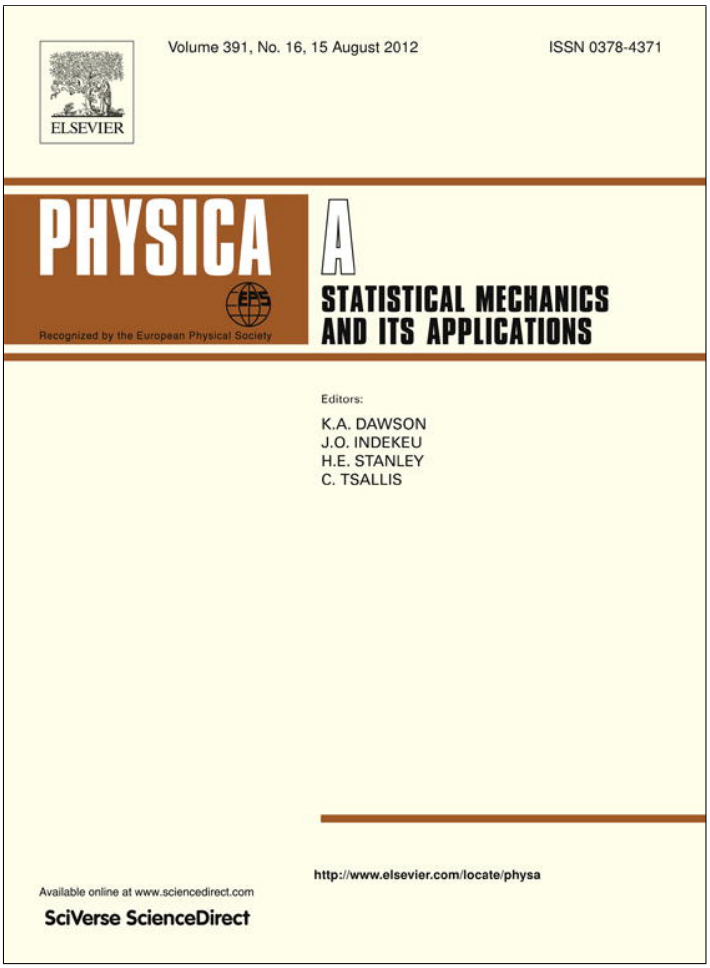

Physica A 391 (2012) 4100–4110

Contents lists available at SciVerse ScienceDirect

Physica A

journal homepage: www.elsevier.com/locate/physa

The effects of observational correlated noises on multifractal detrended fluctuation analysis

Damián Gulich [a,b], Luciano Zunino [a,c,*]

[a] Centro de Investigaciones Ópticas (CONICET La Plata - CIC), C.C. 3, 1897 Gonnet, Argentina

[b] Departamento de Física, Facultad de Ciencias Exactas, Universidad Nacional de La Plata (UNLP), 1900 La Plata, Argentina

[c] Departamento de Ciencias Básicas, Facultad de Ingeniería, Universidad Nacional de La Plata (UNLP), 1900 La Plata, Argentina

ARTICLE INFO

Article history:
Received 20 December 2011
Received in revised form 1 April 2012
Available online 11 April 2012

Keywords:
Multifractality
Multifractal detrended fluctuation analysis
Generalized Hurst exponents
Additive correlated noise
Time series analysis

ABSTRACT

We have numerically investigated the effects that observational correlated noises have on the generalized Hurst exponents, $h(q)$, estimated by using the multifractal generalization of detrended fluctuation analysis (MF-DFA). More precisely, artificially generated stochastic binomial multifractals with increased amount of colored noises were analyzed via MF-DFA. It has been recently shown that for moderate additions of white noise, the generalized Hurst exponents are significantly underestimated for $q < 2$ and they are nearly unchanged for $q \geq 2$ [J. Ludescher, M.I. Bogachev, J.W. Kantelhardt, A.Y. Schumann, A. Bunde, On spurious and corrupted multifractality: the effects of additive noise, short- term memory and periodic trends, Physica A 390 (2011) 2480–2490]. In this paper, we have found that $h(q)$ with $q \geq 2$ are also affected when correlated noises are considered. This is due to the fact that the spurious correlations influence the scaling behaviors associated to large fluctuations. The results obtained are significant for practical situations, where noises with different correlations are inherently present.

1. Introduction

Multifractal properties of time series recorded from observable quantities associated to a system are now extensively studied because of the ubiquity of multifractals in nature. Multiple scaling exponents in the same range of temporal or spatial scales are usually required for a full and appropriate description of the complex dynamics associated with a multifractal system. The accurate estimation of these scaling exponents is fundamental to develop suitable models for simulation and forecasting purposes [1]. The analysis of multifractality from experimental data is a critical task mainly due to the finite size and the discretization of the data record [2,3]. It is worth mentioning that it has been very recently shown that a residual multifractality can appear due to the finite length of the signals and/or due to the long-range correlations present in the time series [4]. It is well-known that the MF-DFA methodology allows a reliable quantification of the multifractal scaling of nonstationary time series [5]. Other methods, such as wavelet transform modulus maxima (WTMM) [6], high-order autocorrelation function [7] and wavelet leaders [8], have been proposed with the same purpose in mind. However, the MF-DFA is widely accepted due to its easy implementation and accurateness. Furthermore, it is recommended in the majority of situations in which the fractal character of data is unknown a priori [9]. Since the seminal paper by Kantelhardt et al. [5] where the MF-DFA technique was introduced, a huge number of applications in different and heterogeneous scientific fields, like seismology [10,11], cosmology [12], biology [13,14], meteorology [15], econophysics [16,17], medicine [18], geophysics [19], epidemiology [20] and music [21–23], without being exhaustive, were published. The MF-DFA methodology

* Corresponding author at: Centro de Investigaciones Ópticas (CONICET La Plata - CIC), C.C. 3, 1897 Gonnet, Argentina.
E-mail addresses: dgulich@ciop.unlp.edu.ar (D. Gulich), lucianoz@ciop.unlp.edu.ar (L. Zunino).

0378-4371/$ – see front matter © 2012 Elsevier B.V. All rights reserved.
doi:10.1016/j.physa.2012.04.001

was generalized to higher dimensions in Ref. [24]. Moreover, the multifractal detrended cross-correlation analysis was recently implemented by Zhou [25] in order to unveil the multifractal behaviors in the power-law cross-correlations between two time series or higher-dimensional quantities recorded simultaneously, generalizing the detrended cross-correlation analysis previously introduced by Podobnik and Stanley [26] and Podobnik et al. [27].

It is clear that experimental data are noisy; the random component can be inherent to the process providing information about the intrinsic dynamics (informative noise) or it can be due to the limited accuracy of the measurement equipment (measurement noise) [28]. Consequently, the analysis of the influence this noise environment has on the multifractal properties of time series is essential. It has been recently studied the performance of MF-DFA in the presence of white additive noise, short-term memory and periodicities [29]. It was found that in the case of moderate amount of completely uncorrelated noise the generalized Hurst exponents for negative moments are considerably underestimated. However, the behavior for large positive moments remains practically unaffected. To consider the measurement noise as white noise, assuming a flat power spectrum and no correlations, is somehow arbitrary because the preliminary filtering in the measurement equipment usually leads to colored noise characterized by a finite power spectrum [28]. The aim of the present paper is to evaluate how additive correlated noises corrupt the multifractality estimated by employing MF-DFA. For that purpose, the generalized Hurst exponents of simulated stochastic binomial multifractal contaminated with different amount of colored noises were analyzed with this approach. As it will be shown below, we find that positive moments are also affected in the correlated case. Moreover, the effect is more pronounced when the correlation of the noise increases. We argue that these findings are relevant for a more proper understanding of the multifractal nature hidden in experimental and natural time series.

The remainder of the paper is organized as follows. In the following section we briefly describe MF-DFA. The numerically generated data used for testing are detailed in Section 3. Our results are presented and discussed in Section 4 and, finally, the findings of this paper are summarized in Section 5.

2. Theoretical backgrounds

MF-DFA [5] is based on the traditional DFA [30]. Given a time series $S = \{x_t, t = 1, \ldots, N\}$, with N being the number of observations, the cumulated data series $Y(i) = \sum_{t=1}^{i} (x_t - \langle x \rangle)$, with $i = 1, \ldots, N$ and $\langle x \rangle = \left(\sum_{t=1}^{N} x_t\right)/N$, is considered. This profile is divided into $\lfloor N/s \rfloor$ nonoverlapping windows of equal length s ($\lfloor a \rfloor$ denotes the largest integer less than or equal to a). Since the record length N does not need to be a multiple of the considered time scale s, a short part at the end of the profile will remain in most cases. Segmentation starts at the very beginning and at the very end of the signal in order to have into account this part of the record; in this way we consider all data with a total of $2\lfloor N/s \rfloor$ windows. A local polynomial fit $y_{\nu,m}(i)$ of degree m is fitted to the profile for each window $\nu = 1, \ldots, 2\lfloor N/s \rfloor$. The degree of the polynomial can be varied in order to eliminate constant ($m = 0$), linear ($m = 1$), quadratic ($m = 2$) or higher order trends of the profile. After that the variance of the detrended time series is evaluated by averaging over all data point i in each segment ν:

$$F_m^2(\nu, s) = \frac{1}{s} \sum_{i=1}^{s} \left\{ Y[(\nu - 1)s + i] - y_{\nu,m}(i) \right\}^2 \tag{1}$$

for $\nu = 1, \ldots, \lfloor N/s \rfloor$ (forward direction) and

$$F_m^2(\nu, s) = \frac{1}{s} \sum_{i=1}^{s} \left\{ Y[N - (\nu - \lfloor N/s \rfloor)s + i] - y_{\nu,m}(i) \right\}^2 \tag{2}$$

for $\nu = \lfloor N/s \rfloor + 1, \ldots, 2\lfloor N/s \rfloor$ (backward direction). An alternative detrending operation by estimating the local trends through empirical mode decomposition has been recently proposed [31].

In order to analyze the influence of fluctuations of different magnitudes and on different time scales, the qth order fluctuation function given by

$$F_q(s) = \left\{ \frac{1}{2\lfloor N/s \rfloor} \sum_{\nu=1}^{2\lfloor N/s \rfloor} \left[F_m^2(\nu, s) \right]^{q/2} \right\}^{1/q} \tag{3}$$

is obtained for a real valued parameter $q \neq 0$. When $q = 0$ a logarithmic averaging procedure has to be employed because of the diverging exponent

$$F_0(s) = \exp\left\{ \frac{1}{4\lfloor N/s \rfloor} \sum_{\nu=1}^{2\lfloor N/s \rfloor} \ln\left[F_m^2(\nu, s) \right] \right\}. \tag{4}$$

For $q = 2$, the standard DFA procedure is retrieved. By construction, $F_q(s)$ is only defined for $s \geq m+2$. As the main purpose is to understand the scaling behavior, the generalized fluctuation functions should be estimated for different values of the time scale s and for different values of the order q.

Generally, if the time series $S = \{x_t, t = 1, \ldots, N\}$ has long-range power-law correlations, $F_q(s)$ scales with s as

$$F_q(s) \sim s^{h(q)} \tag{5}$$

for a certain range of s. The scaling exponents $h(q)$, usually known as generalized Hurst exponents, are estimated by analyzing the double logarithmic plot of $F_q(s)$ versus s for each value of q. In the case of stationary signals, $h(2)$ coincides with the Hurst exponent H. Ideally, for monofractal time series, $h(q)$ are independent of q since the scaling behavior of the variances $F_m^2(\nu, s)$ is identical for all windows ν. Otherwise, a multifractal structure is observed when the scaling behaviors of small and large fluctuations are different. In this case there will be a significant dependence of $h(q)$ with the chosen moment q. The generalized Hurst exponents with negative order q describe the scaling of small fluctuations because the segments ν with small variance will dominate the average $F_q(s)$ for this q-range. Contrarily, for positive order q the windows ν with large variance have stronger influence and, thus, the scaling of large fluctuations is examined. Small fluctuations are usually characterized by larger scaling exponents than those related to large fluctuations.

In this paper, we concentrate on the generalized Hurst exponents description for quantifying the multifractal properties of the time series. Equivalently, the singularity spectrum $(\alpha, f(\alpha))$, sometimes known as Hölder description, could be considered. For details about the link between these two descriptions please see Ref. [1].

3. Numerical data

The binomial multiplicative process is a paradigmatic model for multifractal data [32, Chapter 6]. It was shown that this process fits remarkably well the observed multifractal spectrum of the dissipation field in fully developed turbulence [33]. In the model, a record of length $N = 2^{n_{\max}}$ is constructed recursively in $n_{\max} + 1$ steps. In the generation, a constant time series, i.e. $x_t = 1$ for all $t = 1, \ldots, N$, is constructed. In the first step of the cascade, the first half of the series is multiplied by a factor a and the second half of the series is multiplied by a factor $b = 1 - a$, with the model parameter $a \in \mathbb{R}$ restricted to $0.5 < a < 1$. This procedure is repeated in the next steps. Each series of the previous step is divided into two subseries of equal length, and the left half is multiplied by a and the right half by b until the halves consist of only one element and no more splitting is possible. In this paper we consider the stochastic version of the binomial multiplicative process. The stochastic character is incorporated randomly multiplying in each iteration the left or the right halves by the model parameter a [34]. Note that, in this way, the unrealistic determinism is removed and the underlying multiscaling hierarchy is preserved. This procedure is not equivalent to perform a random permutation of the deterministic model because all the temporal correlations are removed with a shuffled randomization.

The generalized Hurst exponents for both binomial models, deterministic and stochastic, can be theoretically derived. It was shown [5,34] that

$$h(q) = \begin{cases} \dfrac{1}{q}\left(1 - \log_2(a^q + (1-a)^q)\right), & q \neq 0; \\ -\dfrac{1}{2}\left(\log_2 a + \log_2(1-a)\right), & q = 0. \end{cases} \tag{6}$$

Fig. 1 shows completely deterministic and stochastic realizations of the binomial multiplicative multifractal for different values of the model parameter a together with their theoretical generalized Hurst exponents. As can be easily concluded by comparing the generalized Hurst exponents (Fig. 1(g)–(i)), the strength of multifractality ($\Delta h = h(-\infty) - h(+\infty)$)[1] increases and the long-range dependence (i.e., $h(2)$) decreases for higher values of the model parameter. For $a \to 0.5$ the multifractality is principally due to the temporal correlations. With increased values of the parameter ($a \to 1$) the minimum value of the time series, $(1-a)^{n_{\max}}$, is very small compared to the maximum one, $a^{n_{\max}}$, and the broad probability distribution also contributes to the multifractality [9]. It is worth remarking that this multifractal model has only one parameter. Thus, the long-term correlation and multifractality strength cannot be fixed independently of each other. To overcome this drawback, a generalized version of the binomial multiplicative process was proposed [1,34].

4. Results and discussion

In order to understand the influence that additional correlated noises have on the multifractal properties, simulated stochastic binomial multifractals with increased amount of colored noises were analyzed by employing MF-DFA. We have used the Fourier filtering method (FFM) for generating the colored noises. In this numerical algorithm the Fourier transform coefficients of uncorrelated random numbers with a Gaussian distribution are multiplied by $f^{-\beta/2}$. The inverse Fourier transform of this modified coefficients produces a new time series with power spectrum $f^{-\beta}$ [35,29]. Long-range correlated noises with β values between 0 (white noise) and 1 (flicker noise) and step 0.2 were generated. It should be noted that the β scaling exponent and the Hurst exponent H are related through the formula $\beta = 2H - 1$. Furthermore, long-range

[1] For practical applications the multifractal strength is estimated with $\Delta h_q = h(-q) - h(+q)$ for a large value of the order q.

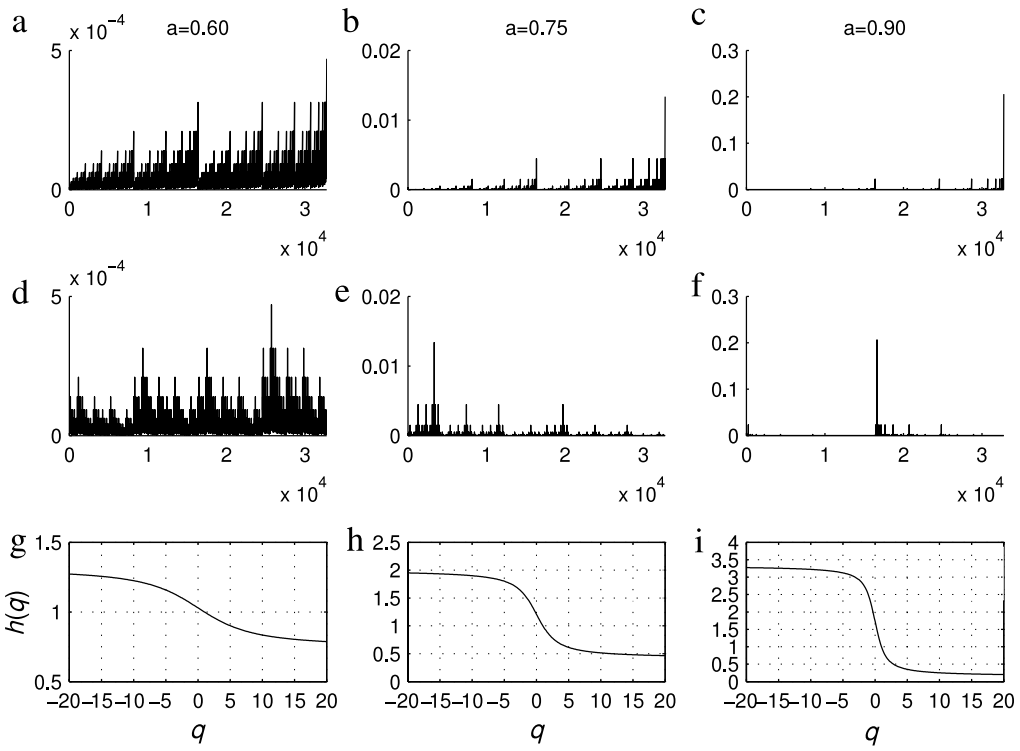

Fig. 1. Numerical simulations of the binomial multiplicative model of length $N = 2^{15}$ data points for different values of the model parameter a for the fully deterministic (a–c) and the stochastic instances (d–f). The generalized Hurst exponents analytically calculated (Eq. (6)) are also plotted (g–i). The long-range dependence and multifractality degree for the different model parameters are the following: $h(2)_{a=0.60} \approx 0.972$, $h(2)_{a=0.75} \approx 0.839$, $h(2)_{a=0.90} \approx 0.643$, $\Delta h_{a=0.60} \approx 0.585$, $\Delta h_{a=0.75} \approx 1.585$ and $\Delta h_{a=0.90} \approx 3.170$.

correlated signals are characterized by a power-law decay of the autocorrelation function $C(\tau) \equiv \langle x_t x_{t+\tau} \rangle = \tau^{-\gamma}$ with $\gamma = 1 - \beta = 2 - 2H$. Consequently, the correlation degree increases for larger β values of the power spectrum. Different noise levels (NL), defined by the standard deviation of the noise divided by the standard deviation of the original signal, were numerically added to the original multifractal signals. One hundred independent realizations of length $N = 2^{15}$ data points were analyzed in each instance and the average results of the generalized Hurst exponents $h(q)$ for q in the range between -20 and 20 with step equal to 0.5 were plotted. Throughout the whole paper, a linear MF-DFA ($m = 1$) was implemented, the fluctuation functions were calculated for time scales $s \in [10, N/4]$, and the scaling behaviors were estimated in the fitting range $s \in [100, 5000]$.

In Figs. 2–10 the generalized Hurst exponents of simulated stochastic binomial multifractal contaminated with different levels of colored noises estimated by employing MF-DFA are plotted. In each figure the model parameter a and the noise level are fixed, and the persistence degree associated with the contaminated noise is increased from top to bottom ($\beta = 0.0, 0.2, \ldots, 1.0$). Figs. 2–4, 5–7 and 8–10 correspond to model parameters $a = 0.60$, 0.75 and 0.90, respectively. Three different noise levels were considered: NL = 0.1 (Figs. 2, 5 and 8), NL = 0.5 (Figs. 3, 6 and 9) and NL = 1.0 (Figs. 4, 7 and 10).

It is clearly observed that generalized Hurst exponents for $q < 2$ are significantly underestimated even in the presence of small additions of noise (correlated or uncorrelated). The effect is more noticeable for larger values of the model parameter ($a = 0.75$ and $a = 0.90$), i.e. for larger multifractality strengths and smaller long-range dependence. The higher robustness to additive noise observed for $a = 0.60$ can be attributed to the fact that the multifractal hierarchy for this model parameter originates from temporal correlations. The multiscaling for $a = 0.75$ and $a = 0.90$ is also related to the fat-tailed probability distributions of the data, and this multifractality source seems to be much more sensitive to additive noise.[2] For a better visualization of these findings, Fig. 11 shows the relative change $\delta_{q=-20} = [h(-20) - h_c(-20)]/h(-20)$ between the edge generalized Hurst exponent estimated values for the original multifractal signal, $h(-20)$, and its contaminated counterpart, $h_c(-20)$, as a function of the β scaling exponent of the spurious added noise. The results obtained for the different model parameters and noise levels are included in the same plot. A clear linear relationship is obtained for $a = 0.90$ independently of the noise intensity. This result is justified taking into account that, for $a = 0.90$ and $q < 0$, $h(q) \approx h_{\text{noise}}$, where h_{noise} is the Hurst exponent of the added long-range correlated noises (please see Figs. 8–10). Thus, for this multifractal model parameter, scalings obtained for negative moments give information about the spurious correlations that corrupt the original multifractal signals. For $a = 0.60$, a maximum deviation is obtained for an intermediate β scaling exponent in the case of

[2] Identifying the source of multiscaling in time series is an elusive issue. Drożdż et al. [3] have recently found that a genuine multifractal hierarchy can only originate from temporal correlations.

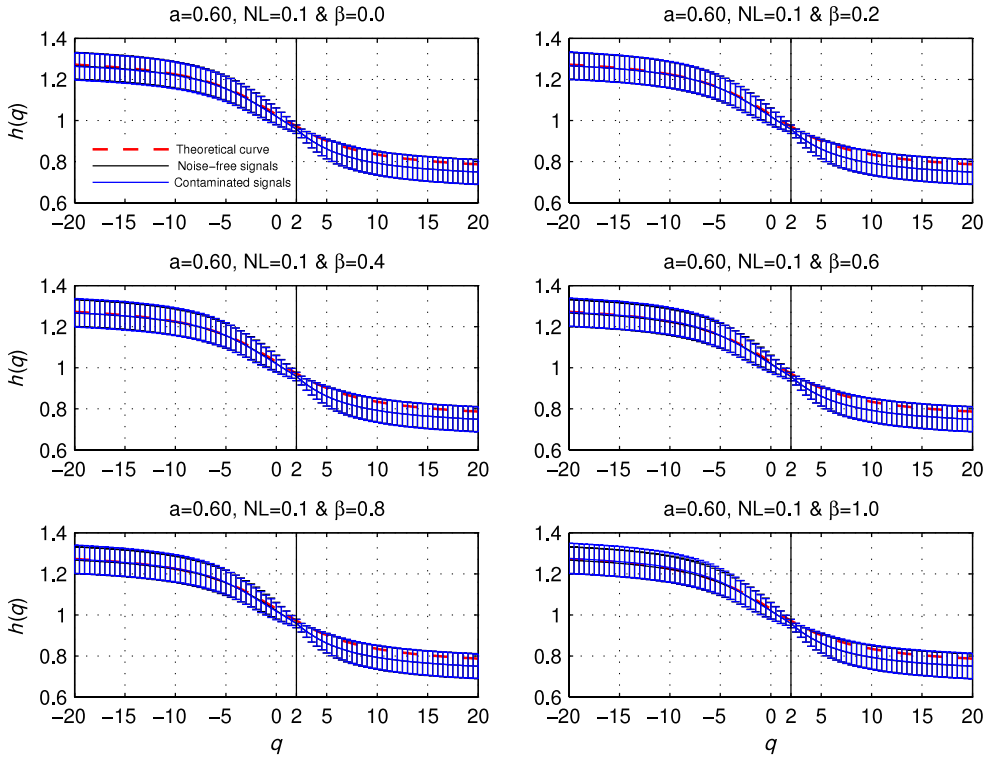

Fig. 2. (Color online) Generalized Hurst exponent of stochastic binomial multifractals with model parameter $a = 0.60$ contaminated with long-range correlated noises with power spectrum $f^{-\beta}$. The noise level was fixed equal to 0.1. Mean and standard deviation estimated from one hundred independent realizations are plotted (blue curves). The results obtained for the noise-free simulations are included for comparison purposes (black curves). The theoretical curve (Eq. (6)) is also depicted (red dashed curves). Vertical black lines are used to identify the case $q = 2$.

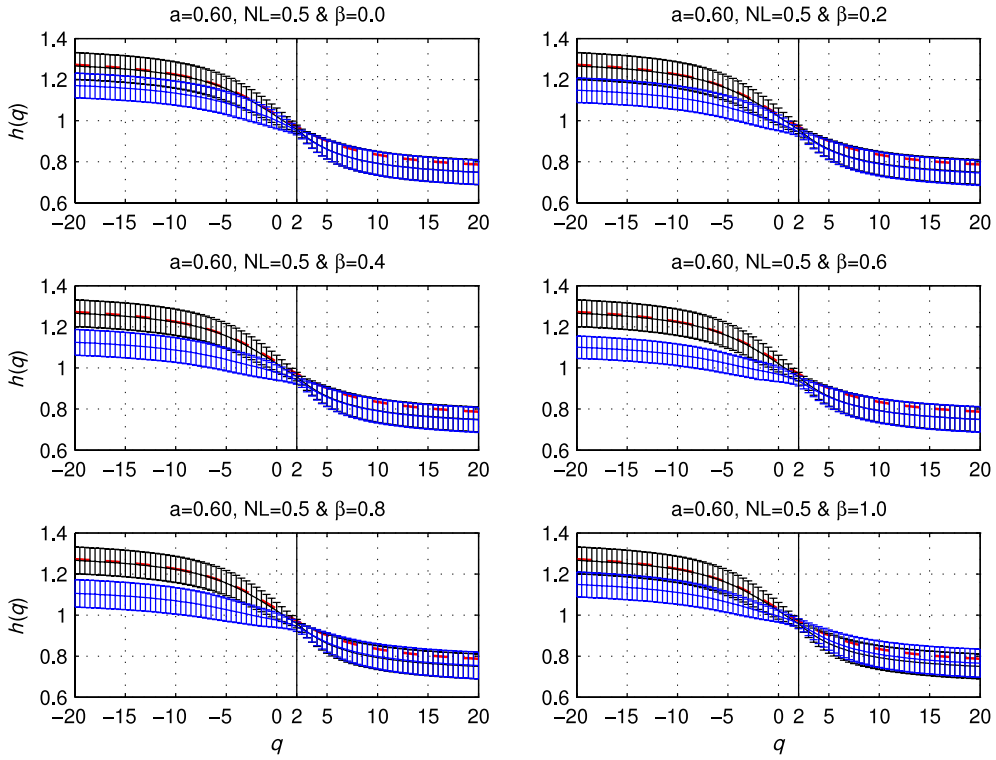

Fig. 3. (Color online) Same as Fig. 3 but for NL = 0.5.

moderate and strong additive noises. We conjecture that the reason behind this interesting effect could be some kind of mixing between the long-range correlations of the signal and those of the colored noise; further work must be done in order

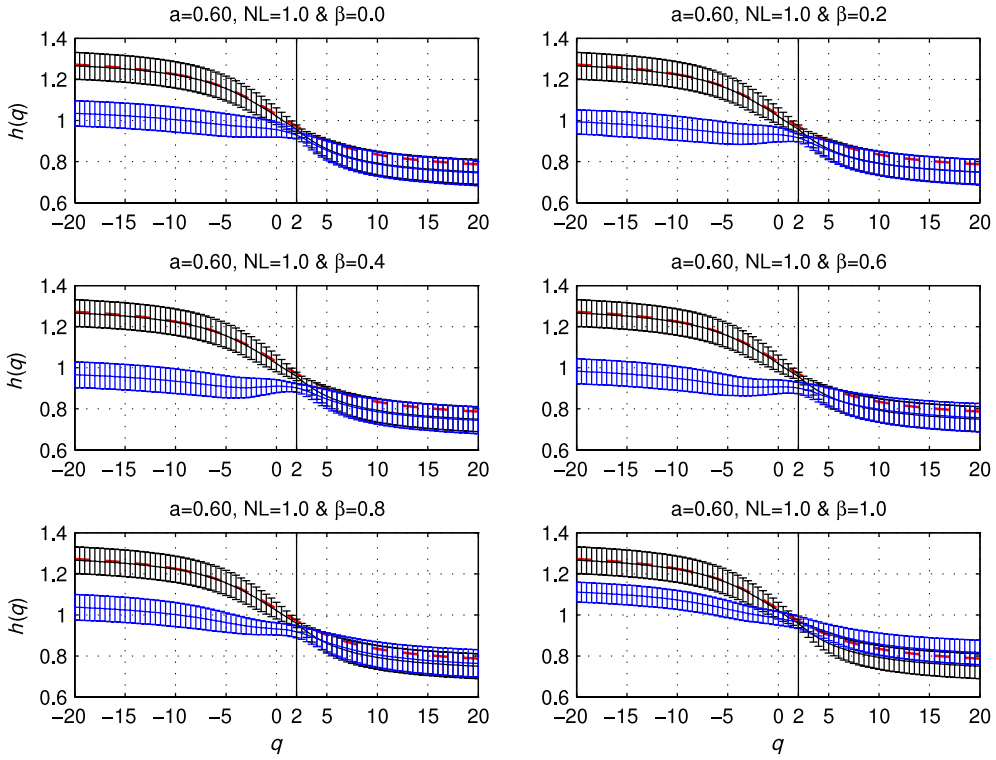

Fig. 4. (Color online) Same as Fig. 3 but for NL = 1.0.

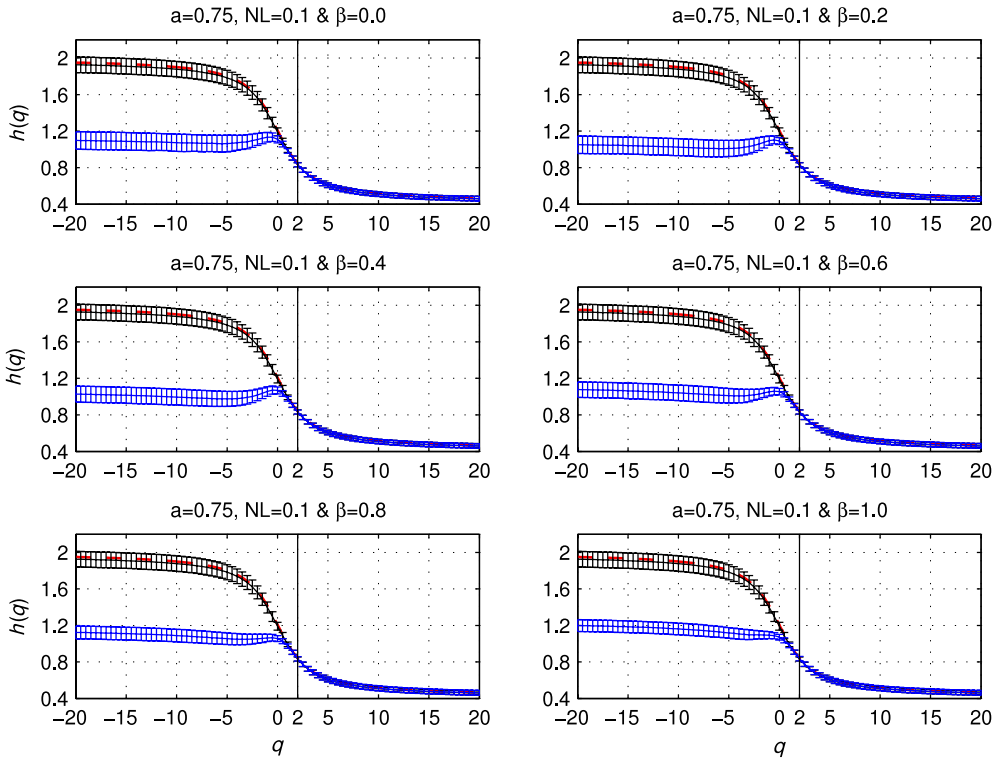

Fig. 5. (Color online) Same as Fig. 3 but for $a = 0.75$ and NL = 0.1.

to confirm this hypothesis. Finally, for $a = 0.75$ an intermediate result is observed, with linear responses for moderate to strong additive noises, and a clear maximum deviation for $\beta = 0.4$ when NL = 0.1.

We have also found that a moderate amount of colored noises (NL = 0.5 and NL = 1.0) prevents a reliable estimation of the scaling exponents for positive moments. This is due to the fact that scalings related to large fluctuations are affected by the long-range correlations present in the colored noises. Obviously, the bias is more pronounced when the long memory of the additive noise increases and a maximum deviation from the expected behavior is observed for the superpersistent case

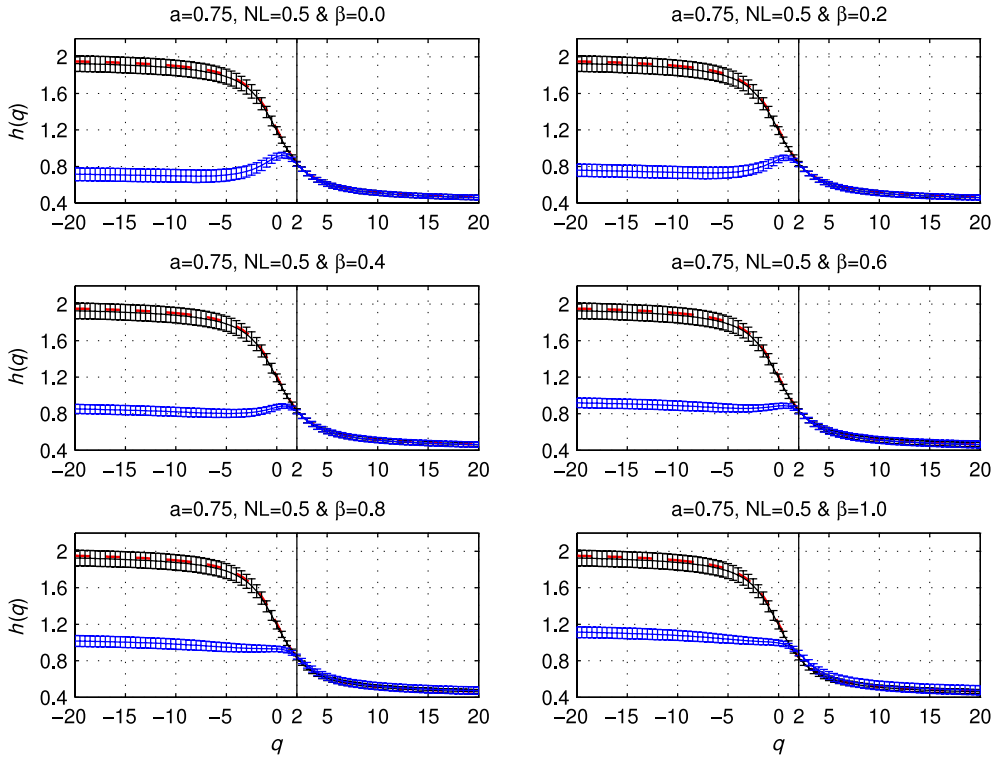

Fig. 6. (Color online) Same as Fig. 3 but for $a = 0.75$ and NL $= 0.5$.

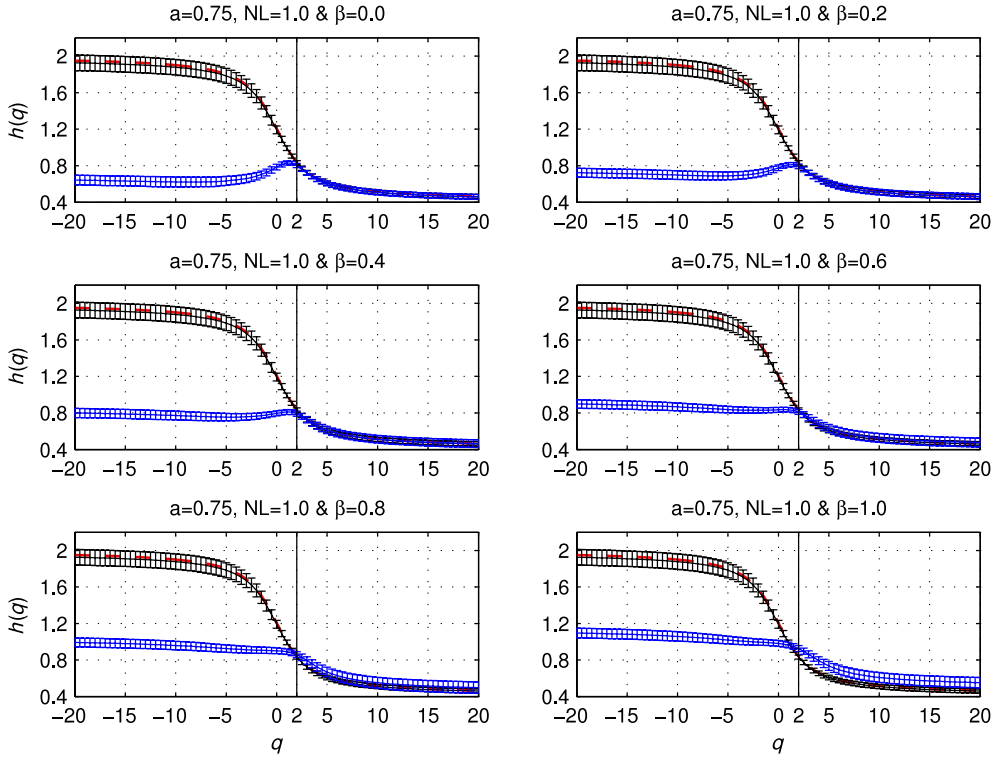

Fig. 7. (Color online) Same as Fig. 3 but for $a = 0.75$ and NL $= 1.0$.

($\beta = 1.0$). This finding is easily concluded from Fig. 12, where the relative change $\delta_{q=2} = [h(2) - h_c(2)]/h(2)$ is depicted as a function of the β scaling exponent of the added noise for the model parameter $a = 0.90$. Consequently, generalized Hurst exponents for $q > 0$ are notably overestimated when the original series are corrupted by additive colored noise.

Trying to shed more light on the reasons behind this spurious effect, Fig. 13 shows the fluctuation functions $F_q(s)$ as a functions of s for $a = 0.90$, NL $= 1.0$ and the different considered colored noises for one randomly chosen realization.

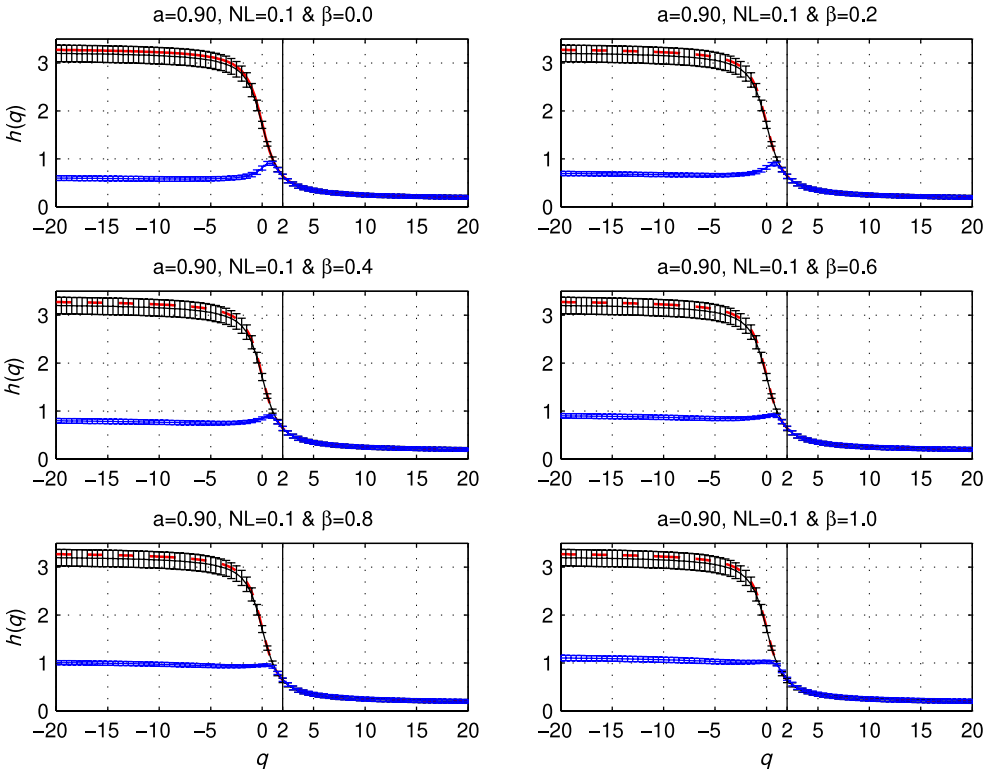

Fig. 8. (Color online) Same as Fig. 3 but for $a = 0.90$ and NL $= 0.1$.

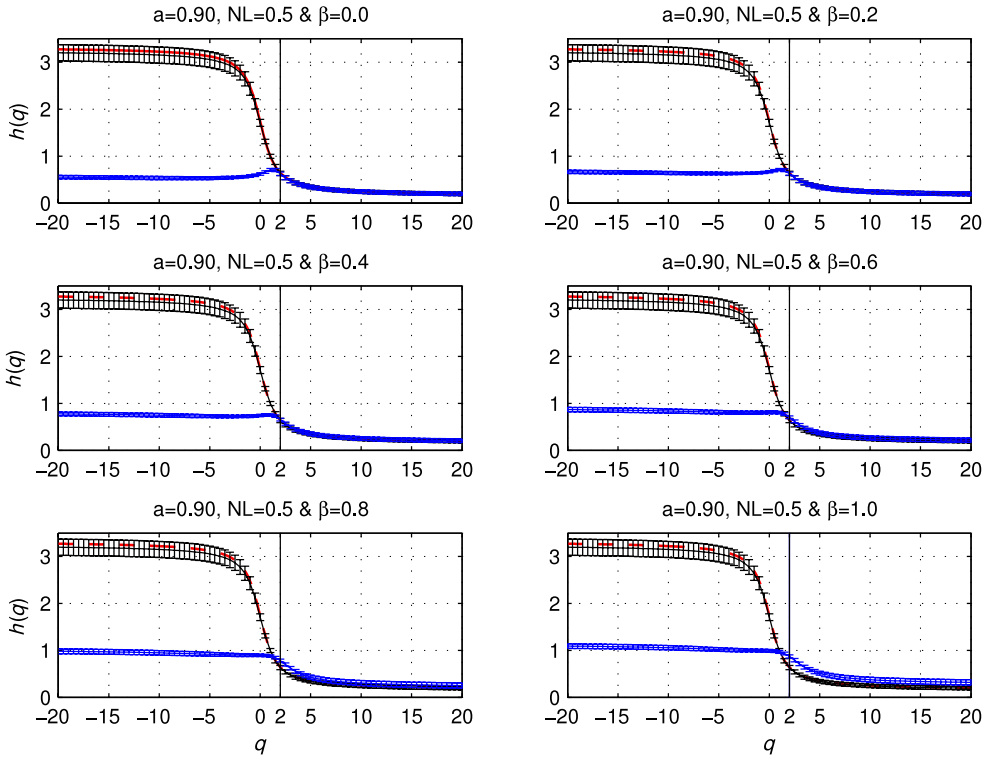

Fig. 9. (Color online) Same as Fig. 3 but for $a = 0.90$ and NL $= 0.5$.

A crossover scale s^* is clearly observed for positive order q when the underlying multifractal time series is corrupted by noises with large correlations ($\beta = 0.6$, $\beta = 0.8$ and $\beta = 1.0$). This particular scale is identified with a vertical black dashed line in Fig. 13(d)–(f). Generalized Hurst exponents with $q > 0$ are overestimated due to this change in the trend. The use of a uniform range of scales for the linear fit is totally questionable in these cases. To be more precise, two distinct regions of scaling, $s < s^*$ and $s > s^*$, must be considered. Moreover, the slopes for the small-scale and large-scale regions appear to be

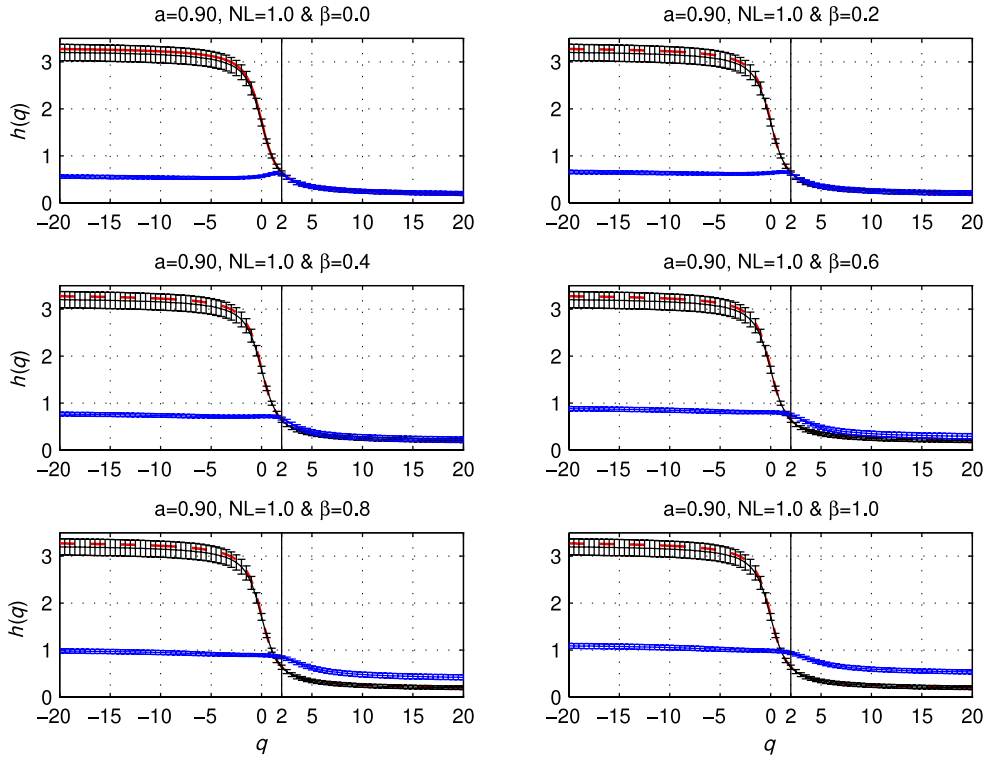

Fig. 10. (Color online) Same as Fig. 3 but for $a = 0.90$ and NL $= 1.0$.

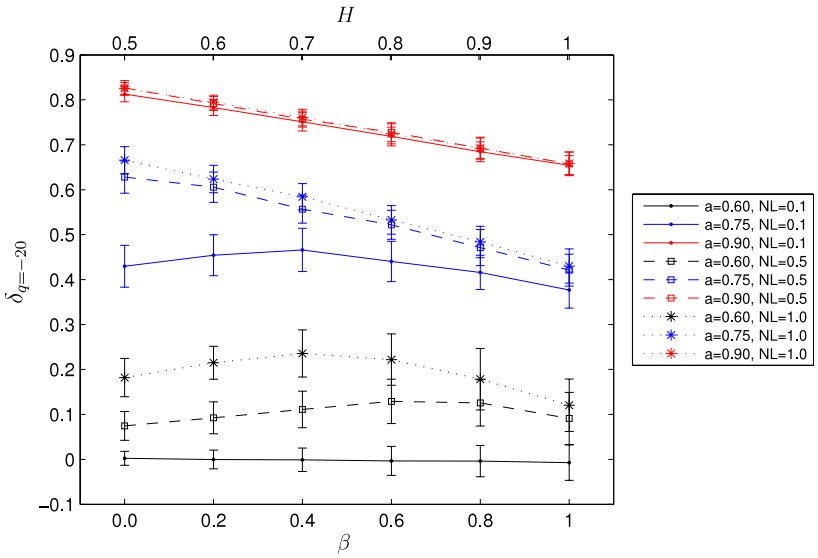

Fig. 11. (Color online) Relative change $\delta_{q=-20} = [h(-20) - h_c(-20)]/h(-20)$ between the edge generalized Hurst exponent estimated values for the original multifractal signal, $h(-20)$, and its contaminated counterpart, $h_c(-20)$, as a function of the β scaling exponent of the spurious added noise for the different model parameters and noise levels. Mean and standard deviation estimated from one hundred independent realizations are plotted.

dependent and independent, respectively, on the order q. This suggests that the scaling on large time scales ($s > s^*$) could be very useful to unveil the nature of the contaminated noise. A systematic estimation of the crossover scale and the two different scaling regimes as a function of the β value and the noise level is beyond the focus of the present paper and will be addressed in a future work.

5. Conclusions

We have found that the spurious effect of additive correlated noises should be properly taken into account when analyzing the multifractal character of experimental data. Generalized Hurst exponents, and, hence, the multifractal spectra estimated by employing the widely used MF-DFA technique can be biased due to the presence of such artifact. On the one hand, $h(q)$ with $q < 2$ are notably underestimated for small amount of additive correlated and uncorrelated noises.

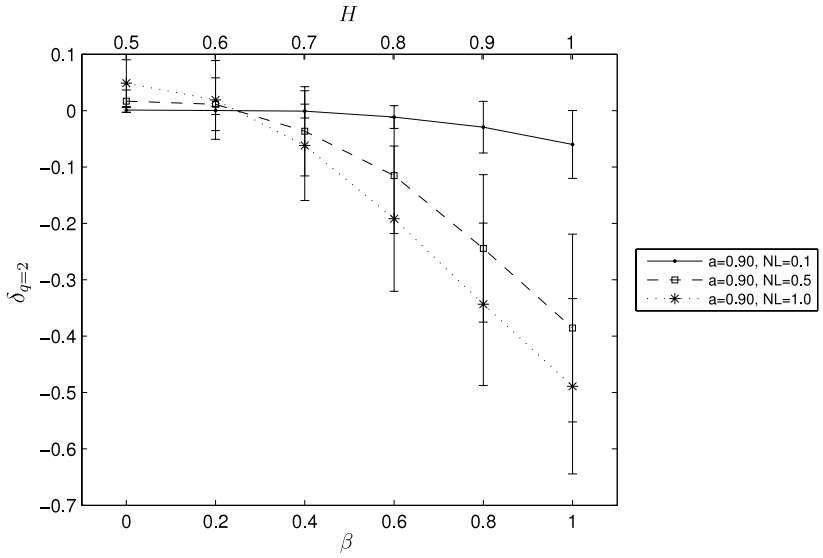

Fig. 12. Relative change $\delta_{q=2} = [h(2) - h_c(2)]/h(2)$ between the Hurst exponent estimations for the original multifractal signal, $h(2)$, and its contaminated counterpart, $h_c(2)$, as a function of the β scaling exponent of the spurious added noise for the model parameter $a = 0.90$. Mean and standard deviation estimated from one hundred independent realizations are plotted.

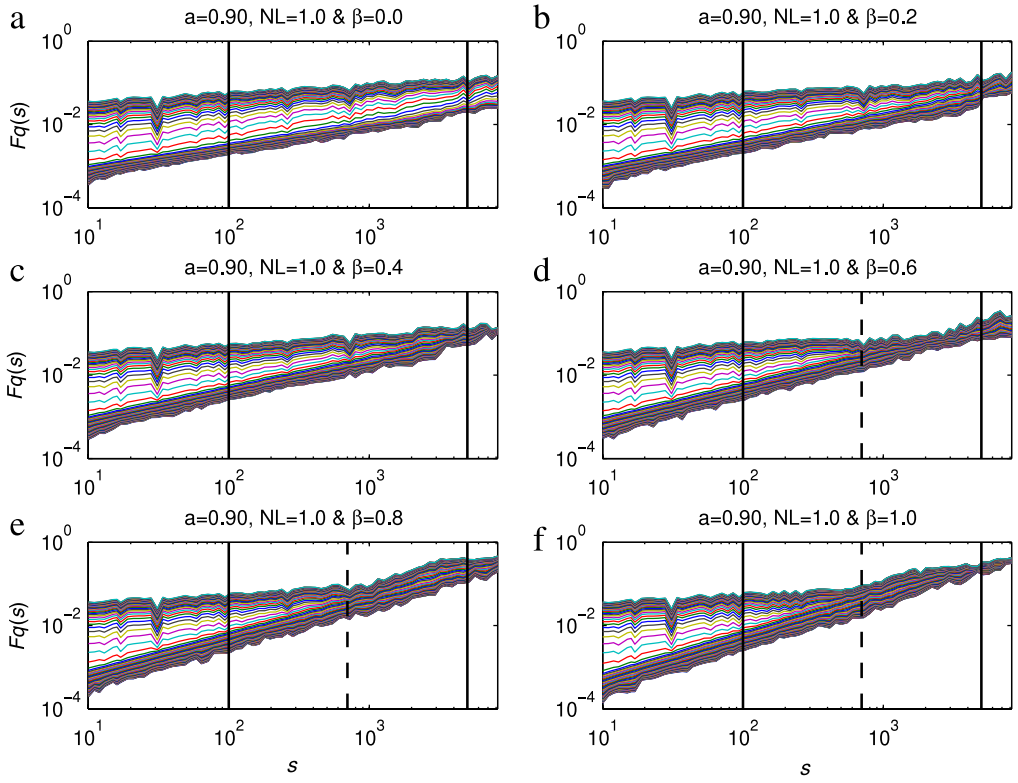

Fig. 13. (Color online) $F_q(s)$ versus s for $a = 0.90$ and NL $= 1.0$ for one realization. The behavior observed is representative for the whole data set. The order q ($q = -20, -19.5, \ldots, 19.5, 20$) increases from bottom to top. Spurious effects related to the different colored noises with power spectrum $f^{-\beta}$ can be better visualized. Vertical black solid lines are included to indicate the fitting range. Vertical black dashed line marks the crossover scale s^* observed for positive q when the original multifractal signal is contaminated with noises with large correlations.

On the other hand, moderate additions of colored noises also affect $h(q)$ with $q \geq 2$. More precisely, the generalized Hurst exponents in this q-range are overestimated and the bias is more significant when the correlation of the noise increases. It is clear that the long-range correlations present in the noises have an influence on the scaling behaviors associated to large fluctuations. Thus, positive moments result affected. Taking into account that correlated noises are inherently present in experimental data, the results obtained can be useful for unveiling multifractal features in practical situations. A comparison with the performance of other practical methods to quantify multifractality, like WTMM, in a noise environment and the confirmation of the lower sensitivity to observational noise observed for Gaussian multifractals are promising tasks for the future.

Acknowledgments

We thank the anonymous reviewers for their useful comments and suggestions that helped to improve an earlier version of this paper. Damián Gulich and Luciano Zunino were supported by Consejo Nacional de Investigaciones Científicas y Técnicas (CONICET), Argentina.

References

[1] J.W. Kantelhardt, Fractal and multifractal time series, in: R.A. Meyers (Ed.), Encyclopedia of Complexity and Systems Science, Springer, 2009.
[2] A. Turiel, C.J. Pérez-Vicente, J. Grazzini, Numerical methods for the estimation of multifractal singularity spectra on sampled data: a comparative study, J. Comput. Phys. 216 (2006) 362–390.
[3] S. Drożdż, J. Kwapień, P. Oświęcimka, R. Rak, Quantitative features of multifractal subtleties in time series, Europhys. Lett. 88 (2009) 60003.
[4] D. Grech, G. Pamuła, Multifractal background noise of monofractal signals, Acta Phys. Pol. A 121 (2012) B34–B39.
[5] J.W. Kantelhardt, S.A. Zschiegner, E. Koscielny-Bunde, S. Havlin, A. Bunde, H.E. Stanley, Multifractal detrended fluctuation analysis of nonstationary time series, Physica A 316 (2002) 87–114.
[6] J.F. Muzy, E. Bacry, A. Arneodo, Wavelets and multifractal formalism for singular signals: application to turbulence data, Phys. Rev. Lett. 67 (1991) 3515–3518.
[7] A.-L. Barabási, P. Szépfalusy, T. Vicsek, Multifractal spectra of multi-affine functions, Physica A 178 (1991) 17–28.
[8] E. Serrano, A. Figliola, Wavelet leaders: a new method to estimate the multifractal singularity spectra, Physica A 388 (2009) 2793–2805.
[9] P. Oświęcimka, J. Kwapień, S. Drożdż, Wavelet versus detrended fluctuation analysis of multifractal structures, Phys. Rev. E 74 (2006) 016103 (17 pages).
[10] L. Telesca, V. Lapenna, M. Macchiato, Multifractal fluctuations in seismic interspike series, Physica A 354 (2005) 629–640.
[11] L. Telesca, V. Lapenna, Measuring multifractality in seismic sequences, Tectonophysics 423 (2006) 115–123.
[12] M. Sadegh Movahed, F. Ghasemi Sohrab Rahvar, M. Reza Rahimi Tabar, Long-range correlation in cosmic microwave background radiation, Phys. Rev. E 84 (2011) 021103 (9 pages).
[13] P.H. Figueirêdo, E. Nogueira Jr., M.A. Moret, S. Coutinho, Multifractal analysis of polyalanines time series, Physica A 389 (2010) 2090–2095.
[14] S. Dutta, Multifractal properties of ECG patterns of patients suffering from congestive heart failure, J. Stat. Mech. 12 (2010) P12021.
[15] I.T. Pedron, Correlation and multifractality in climatological time series, J. Phys. Conf. Ser. 246 (2010) 012034.
[16] L. Zunino, B.M. Tabak, A. Figliola, D.G. Pérez, M. Garavaglia, O.A. Rosso, A multifractal approach for the stock market inefficiency, Physica A 387 (2008) 6558–6566.
[17] L. Zunino, A. Figliola, B.M. Tabak, D.G. Pérez, M. Garavaglia, O.A. Rosso, Multifractal structure in Latin-American market indices, Chaos, Solitons Fractals 41 (2009) 2331–2340.
[18] F. Liao, Y.-K. Jan, Using multifractal detrended fluctuation analysis to assess sacral skin blood flow oscillations in people with spinal cord injury, J. Rehabil. Res. Dev. 48 (2011) 787–799.
[19] F.A. Hirpa, M. Gebremichael, T.M. Over, River flow fluctuation analysis: effect of watershed area, Water Resour. Res. 46 (2010) W12529 (10 pages).
[20] Y. Leung, E. Ge, Z. Yu, Temporal scaling behavior of avian influenza A (H5N1): the multifractal detrended fluctuation analysis, Ann. Assoc. Am. Geographers 101 (2011) 1221–1240.
[21] G.R. Jafari, P. Pedram, L. Hedayatifar, Long-range correlation and multifractality in Bach's inventions pitches, J. Stat. Mech. (2007) P04012.
[22] L. Telesca, M. Lovallo, Revealing competitive behaviours in music by means of the multifractal detrended fluctuation analysis: application to Bach's Sinfonias, Proc. R. Soc. A 467 (2011) 3022–3032.
[23] P. Oświęcimka, J. Kwapień, I. Celińska, S. Drożdż, R. Rak, Computational approach to multifractal music, 2011. ArXiv:1106.2902v1 [physics.data-an].
[24] G.-F. Gu, W.-X. Zhou, Detrended fluctuation analysis for fractals and multifractals in higher dimensions, Phys. Rev. E 74 (2006) 061104 (8 pages).
[25] W.-X. Zhou, Multifractal detrended cross-correlation analysis for two nonstationary signals, Phys. Rev. E 77 (2008) 066211 (4 pages).
[26] B. Podobnik, H.E. Stanley, Detrended cross-correlation analysis: a new method for analyzing two nonstationary time series, Phys. Rev. Lett. 100 (2008) 084102 (4 pages).
[27] B. Podobnik, D. Horvatic, A.M. Petersen, H.E. Stanley, Cross-correlations between volume change and price change, PNAS 106 (2009) 22079–22084.
[28] M.I. Bogachev, A. Bunde, On the predictability of extreme events in records with linear and nonlinear long-range memory: efficiency and noise robustness, Physica A 390 (2011) 2240–2250.
[29] J. Ludescher, M.I. Bogachev, J.W. Kantelhardt, A.Y. Schumann, A. Bunde, On spurious and corrupted multifractality: the effects of additive noise, short-term memory and periodic trends, Physica A 390 (2011) 2480–2490.
[30] C.-K. Peng, S.V. Buldyrev, S. Havlin, M. Simons, H.E. Stanley, A.L. Goldberger, Mosaic organization of DNA nucleotides, Phys. Rev. E 49 (1994) 1685–1689.
[31] X.-Y. Qian, G.-F. Gu, W.-X. Zhou, Modified detrended fluctuation analysis based on empirical mode decomposition for the characterization of anti-persistent processes, Physica A 390 (2011) 4388–4395.
[32] J. Feder, Fractals, Plenum Press, New York, 1988.
[33] C. Meneveau, K.R. Sreenivasan, Simple multifractal cascade model for fully developed turbulence, Phys. Rev. Lett. 59 (1987) 1424–1427.
[34] A.Y. Schumann, J.W. Kantelhardt, Multifractal moving average analysis and test of multifractal model with tuned correlations, Physica A 390 (2011) 2637–2654.
[35] H.A. Makse, S. Havlin, M. Schwartz, H.E. Stanley, Method for generating long-range correlations for large systems, Phys. Rev. E 53 (1996) 5445–5449.